AMERICAN SCIENTIFIC PUBLISHERS

Science of Advanced Materials
Vol. 13, pp. 1498–1505, 2021
www.aspbs.com/sam

ARTICLE

Improved Electrical and Optical Properties of Ultra-Thin Tin Doped Indium Oxide (ITO) Thin Films by a 3-Dimensionally Confined Magnetron Sputtering Source

Long Wen[1], Bibhuti-B Sahu[3], Jeon-Geon Han[1,*], and Geun-Young Yeom[1,2,*]

[1]*School of Advanced Materials Science and Engineering, Sungkyunkwan University, 2066, Seobu-ro, Jangan-gu, Suwon-si, Gyeonggi-do 16419, Republic of Korea*
[2]*SKKU Advaced Institute of Nano Technology (SAINT), Sungkyunkwan University, 2066, Seobu-ro, Jangan-gu, Suwon-si, Gyeonggi-do 16419, Republic of Korea*
[3]*Department of Energy Science and Engineering, IIT Delhi 110016, India*

ABSTRACT

The ultra-thin tin doped crystalline indium oxide (ITO) films (≤50 nm) were successfully deposited by a 3-dimensionally confined magnetron sputtering source (L-3DMS) at the temperature lower than 100 °C. The resistivity and the mobility of the ultra-thin ITO films deposited at a low processing temperature were about $\sim 5 \times 10^{-4}\ \Omega \cdot$cm and >30 cm^2/Vs, respectively, for the thickness of 30 nm. The high quality of the ultra-thin ITO films deposited by L-3DMS is believed to be related to the improved crystallinity with oxygen vacancies of the ITO films by high density plasma and low discharge voltage of the L-3DMS which enables the formation of a crystalline structure a low processing temperature.

KEYWORDS: Transparent Conducting Oxide (TCO), 3-D Confined Magnetron Sputtering, ITO Film, High Plasma Density, Crystal Structure, Low Temperature.

1. INTRODUCTION

Over the past few decades, the tin doped indium oxide (ITO) has been a leading transparent conductive material for the various applications such as flat panel displays, solar cells, smart windows, gas sensors, organic light emitting devices, etc.[1,2] It is well known that the ITO thin film with a crystalline structure $(1\sim3 \times 10^{-4}\ \Omega \cdot \text{cm})$[3] is better than an amorphous structure $(6\sim9 \times 10^{-4}\ \Omega \cdot \text{cm})$.[4,5] The amorphous structure ITO films are reported to have a high resistivity due to the absence of tin (Sn) dopant activation[6] while the ITO films with the crystalline structure are reported to show a low resistivity because it is doped by the substitution of Sn^{4+} into In^{3+} sites by the presence of oxygen vacancies.[7] That is, for the amorphous structured ITO thin films, Sn is not efficiently activated and the carriers are contributed primarily to oxygen vacancies. The state of ITO thin films structure is dependent on processing variables such as substrate temperature, film thickness, etc. According to previous researches,[8–11] the ITO film is an amorphous structure when the deposited thickness is thin (up to 100∼200 nm in thickness) and at a low processing temperature. On the contrary, the ITO film is a crystalline structure when the deposited film thickness is high (above 200 nm in thickness) and at the substrate temperature above 150 °C. The high substrate temperature and thick thickness for crystalline ITO film are the drawbacks for the applications to flexible displays because the thick ITO films are brittle for flexible substrates and high temperature processing damages the substrate. Therefore, for display applications, the key issue of ITO films is to synthesize a crystalline thin film at a low temperature.

ITO thin films have been deposited by various methods likes ion beam sputtering,[12] pulsed laser deposition,[13] spray pyrolysis,[12] electron beam evaporation,[14] sol–gel process,[15] chemical vapor deposition,[16] DC and RF magnetron sputtering,[17,18] etc. Among these methods, DC magnetron sputtering is widely used methods, due to the good uniformity and high quality thin film can be deposited over a large area. Moreover, DC magnetron sputtering has high deposition rates and the deposited film property can be easily controlled by adjusting plasma parameters such as power, pressure, inert gas flow rate, etc. Crystalline ITO thin films can be also deposited by DC magnetron sputtering at high substrate temperatures. However, for flexible displays, the substrate temperature

*Authors to whom correspondence should be addressed.
Emails: jghan@skku.edu, gyyeomskku.edu
Received: 25 April 2021
Accepted: 25 June 2021

is limited due to the use of polymer materials as the substrates, thus, the formation crystalline ultra-thin ITO films by DC magnetron sputtering at a low temperature without annealing will be challenging.

In a previous research, a high density plasma magnetron source which is called the 3D confined magnetron source (3DMS) has been developed.[19, 20] The 3DMS can generate low energy and high ion flux to the substrate by efficient inelastic energy transfer between the electron and neutrals via collisions. In this study, a modified version of 3D magnetron source (scale-up 3-dimensionally confined magnetron sputtering source; L-3DMS) was used to deposit highly electrical property and ultra-thin ITO films at a low temperature and the effects of process conditions on the deposited ultra-thin ITO properties were investigated. Also, correlations between the measured deposited ITO film properties and plasma characteristics were investigated.

2. EXPERIMENTAL DETAILS

The large area 3D magnetron source (L-3DMS) was installed at the top of a stainless-steel cylindrical vacuum chamber (the length–700 mm, the inner diameter–490 mm). Figure 1 shows the schematic drawing of the detailed experimental system composed of a vacuum chamber, the L-3DMS, and an analysis tool. The L-3DMS was made of five planar and rectangular magnetron sources attached with 4 mm thick ITO targets. The figure denotes the X–Z plane and Y–Z plane as shorter and the longer sides of magnetron targets, respectively. In the longer sides, two target parallel to each other, and dimensions of 300×80 mm and the shorter sides with the dimensions of 200×80 mm. Additionally, the fifth target which is placed at the top side (X–Y plan) has the target dimensions of 300×200 mm. This special construction forms more completely confined magnetic fields and traps more high energy electrons, and it leads to a high density plasma.

The ultra-thin ITO film was deposited on the glass and silicon substrates at room temperature without any intentional substrate heating with an ITO target of 10 wt.% Sn_2O_3/90 wt.% In_2O_3 ceramic target. DC power (Advanced Energy, DC Pinnacle) was applied to the magnetron targets while flowing Ar(110 sccm)/O_2(0~0.4 sccm) at a constant working pressure of 4 mTorr. The distance between the substrate and target was 60 mm. Before the deposition, the substrates were used to acetone and alcohol for cleaning. After cleaning, the substrates were placed at the center of the substrate holder.

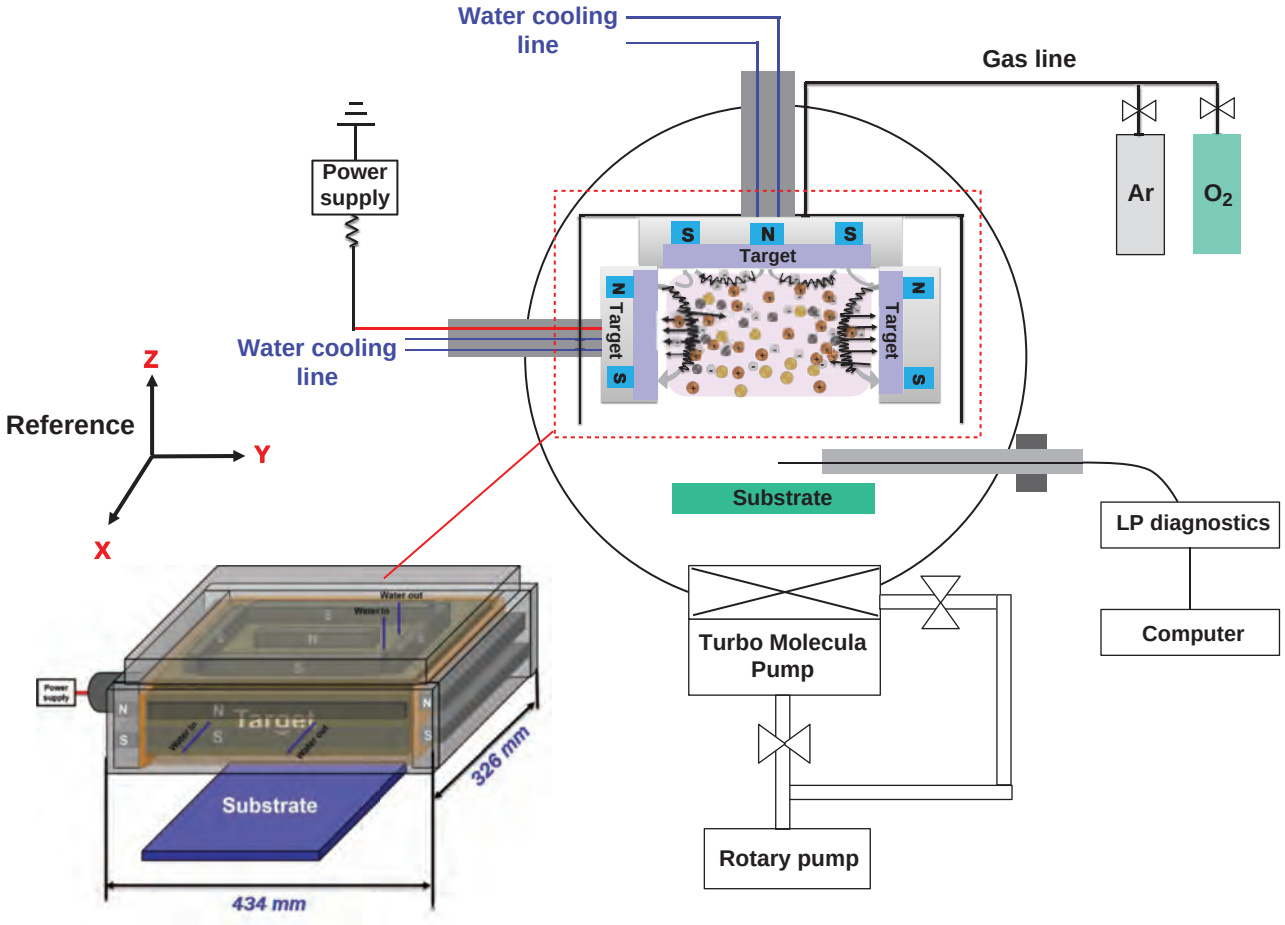

Fig. 1. Schematic representation of the L-3DMS used in the experiment.

ARTICLE

The chambers base pressure was less than 5×10^{-6} Torr using a turbo molecular pump (Osaka Vacuum, TG1100F) backed by a rotary pump (Edwards Vacuum, E2M80) and a booster (Edwards Vacuum, EH250).

The current-voltage (I–V) characteristics of the magnetron source were measured to study the capability of the L-3DMS. A Langmuir probe (LP) inserted from the side port of the chamber was used to analysis of plasma parameters such as plasma potential (V_p), electron temperature (T_e) and plasma density (n_o).[21] The deposited films thickness was measured using a step profilometer (Alpha step; D-500 Stylus). The structural information of the deposited films was obtained using High Resolution X-ray Diffraction (XRD) with a Cu Kα ($\lambda = 1.5418$ Å) source with the scanning range between $2\theta = 20$ and 80°. X-ray photoelectron spectroscopy (XPS; MultiLab 2000) was used to characterize the bonding information of In, Sn, and O. Aluminum K_α (1486.6 eV) radiation was used as the XPS measurements and the XPS core-level spectra were calibrated with the C 1 *s* peak at 284.6 eV as the reference. The optical transmittance of the deposited ITO film was obtained using a UV-visible spectrophotometer (UV-1800 ENG 240 V SOFT) for the 200∼800 nm wavelength range. The deposited ITO films electrical properties were measured by Hall-effect measurement (ECOPIA HMS-3000) and a 4-point probe at room temperature.

3. RESULTS AND DISCUSSION

Figure 2(a) shows the measured discharge current-discharge voltage (I–V) characteristics of the L-3DMS operated with increasing DC power for various Ar operating pressures. As shown, the operating voltage was generally lower than the voltage of conventional magnetron sputtering[22] by showing 200∼400 V due to the strong magnetic field confinement of the L-3DMS.[23] In addition, high discharge currents due to the high plasma density in addition to large cathode area of the L-3DMS were observed, and which will assist high sputtering rate of ITO films by the L-3DMS. The I–V characteristics as a function of oxygen flow rate between 0 and 0.4 sccm at 4 mTorr of Ar (110 sccm) were also observed, but no significant change in I–V characteristics could be observed (not shown) even though the characteristics of the deposited ITO are significantly varied (discussed later). Figure 2(b) shows the characteristics of the L-3DMS plasmas measured by a LP at the substrate position with increasing DC power to the L-3DMS. As shown, with increasing power density (1.0 W/cm^2 corresponds to 800 W) from 1.0 to 3.0 W/cm^2, the plasma density (n_o) was increased from 0.55 to 4.1 $\times 10^{11}$ cm^{-3} while the electron temperature (T_e) near the substrate was increased from 1.7 to 2.6 eV. Due to the increase of electron temperature with increasing the power density, the plasma potential (V_p) was also increased with increasing the power density, however, due to the low electron temperatures, the plasma potentials on the substrate were also generally low and were in the range of 4∼7 V. The high plasma densities observed for L-3DMS is believed to be due to the strong confinement of the high energy electrons near the magnetron surface. The ITO deposition rate measured with increasing the power density is shown in Figure 2(c), and due to the high plasma density, the deposition rate was generally high at a given power density by showing a deposition rate of 115 nm/min at the power density of 3 W/cm^2. This deposition rate was not noticeably changed when a small oxygen flow rate of 0∼0.4 sccm was added to Ar.

Figures 3(a) and (b) show that details of electrical (resistivity, carrier concentration, and mobility) and microstructural characteristics of the deposited 30 nm thick ultra-thin ITO films, respectively, measured a function of oxygen flow rate to Ar at 3 W/cm^2 of power density. With increasing the oxygen flow rate from 0 to 0.2 sccm, the resistivity was initially decreased from 7.4×10^{-4} to 5.2×10^{-4} $\Omega \cdot$cm, however, the further increase of oxygen flow rate to 0.4 sccm increased the resistivity. In the case of carrier concentration, the initial increase of oxygen flow rate from 0 to 0.2 sccm increased the carrier concentration

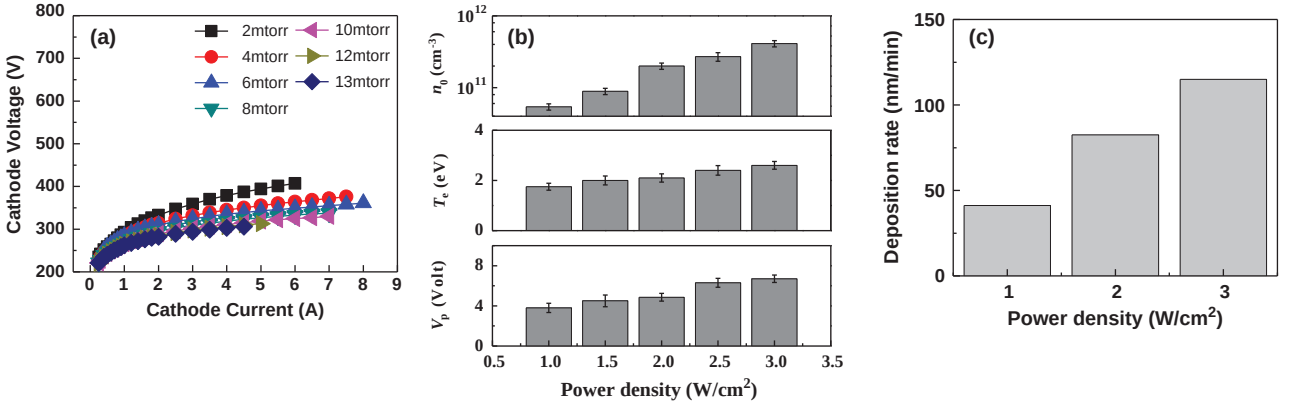

Fig. 2. Characteristics of the L-3DMS. (a) current-voltage curve as a function of operating pressure. (b) plasma characteristics near the substrate location and (c) ITO deposition rate as a function of power density at 4 mTorr of Ar operating pressure.

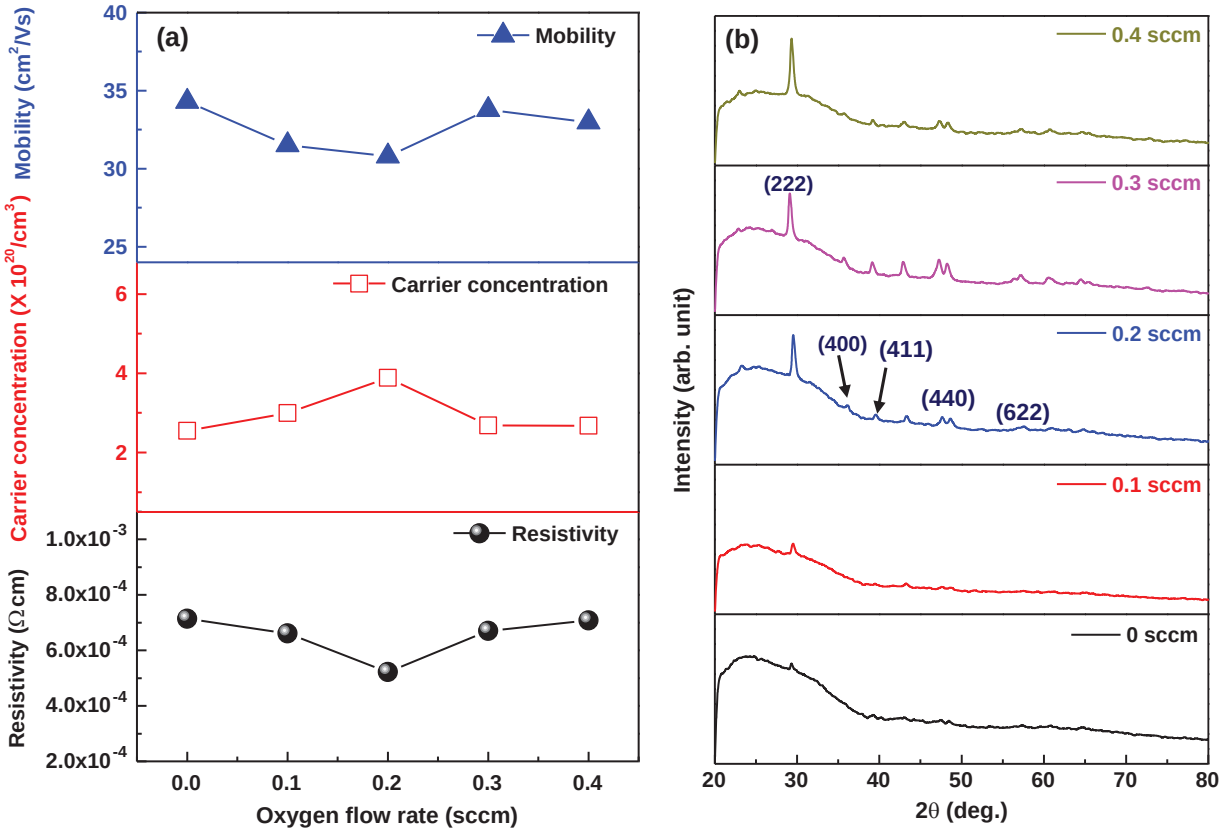

Fig. 3. (a) Electrical characteristics (resistivity, carrier concentration, and mobility) and (b) XRD spectra of the 30 nm thick ultra-thin ITO films deposited as a function of oxygen flow rate at 4 mTorr Ar and 3 W/cm^2 of power density.

from 2.5×10^{20} to 3.8×10^{20} cm^{-3} and the further increase of oxygen flow rate decreased the carrier concentration. The variation of mobility was similar to that of resistivity but the change was smaller by showing the value in the range of 31∼34.3 cm^2/Vs (decrease from 34.3 to 31 cm^2/Vs when the oxygen flow rate is increased from 0 to 0.2 sccm and increase to∼33 when oxygen flow rate is further increased to 0.4 sccm.). The microstructure information measured by the XRD in Figure 3(b) shows that 30 nm thick ultra-thin ITO films have crystalline structures for the oxygen flow rate equal to/higher than 0.2 sccm by showing a high intensity crystalline peak of (222) plane and other XRD peaks are corresponding to (622), (440), (411) and (400) planes of ITO crystalline reflecting the In_2O_3 bixbyite structure.[24]

Using XPS, the narrow scan data of In $3d_{5/2}$ and Sn $3d_{5/2}$ were observed for different oxygen flow rate for the conditions in Figure 3 and the results are shown in Figures 4(a) and (b), respectively. In the case of XPS peak of In $3d_{5/2}$, the peak position was varied from 444.37 eV (0 sccm O_2) to 444.21 eV (0.2 sccm O_2), and to 444.41 eV (0.4 sccm O_2). It is reported that the binding peak energies of 445.24 eV (solid line) and 444.1 eV (dotted line) are attributed to In $3d_{5/2}$ peaks of amorphous ITO and the crystalline ITO, respectively,[25] possibly indicating more crystalline structure for the deposition condition of 0.2 sccm oxygen flow rate similar to the results obtained by XRD in Figure 3(b). In the case of XPS narrow scan data of Sn $3d_{5/2}$, as shown in Figure 4(b), the binding peaks are located at 486.26 eV for 0 sccm/0.4 sccm of oxygen flow rates and at 486.18 eV for 0.2 sccm of oxygen flow rate. The Sn $3d_{5/2}$ peaks at 487.0 eV (solid line) and 486.2 eV (dotted line) are known to be related to the peaks of Sn^{2+} and Sn^{4+}, respectively. Therefore, the Sn $3d_{5/2}$ peaks observed for oxygen flow rates of 0∼0.4 sccm are related to the binding energies of crystalline Sn^{4+} which can be more electrically active dopant.[26] However, the Sn $3d_{5/2}$ peaks, it is not significantly different at all oxygen flow rate conditions.

By measuring oxygen XPS narrow scan data of O 1 s and by deconvoluting into two peaks at the energies 530.1 eV (O_I) and 531.7 eV (O_{II}) (not shown), the peak intensity ratios of O_{II}/O_I were obtained and the results are shown in Figure 4(c) for different oxygen flow rate conditions in Figure 3. The two peaks of at the energies 530.1 eV (O_I) and 531.7 eV (O_{II}) are known to be related to the doubly-charged O^{2-} ions in the crystalline phase without oxygen defect and the oxygen with a neighbor oxygen defect (neighbor oxygen atom is vacant) of In_2O_3, respectively.[27] Therefore, the intensity ratio of O_{II}/O_I in Figure 4(c) shows the ratio of oxygen vacancies in the deposited films. As shown in Figure 4(c), the ratio was

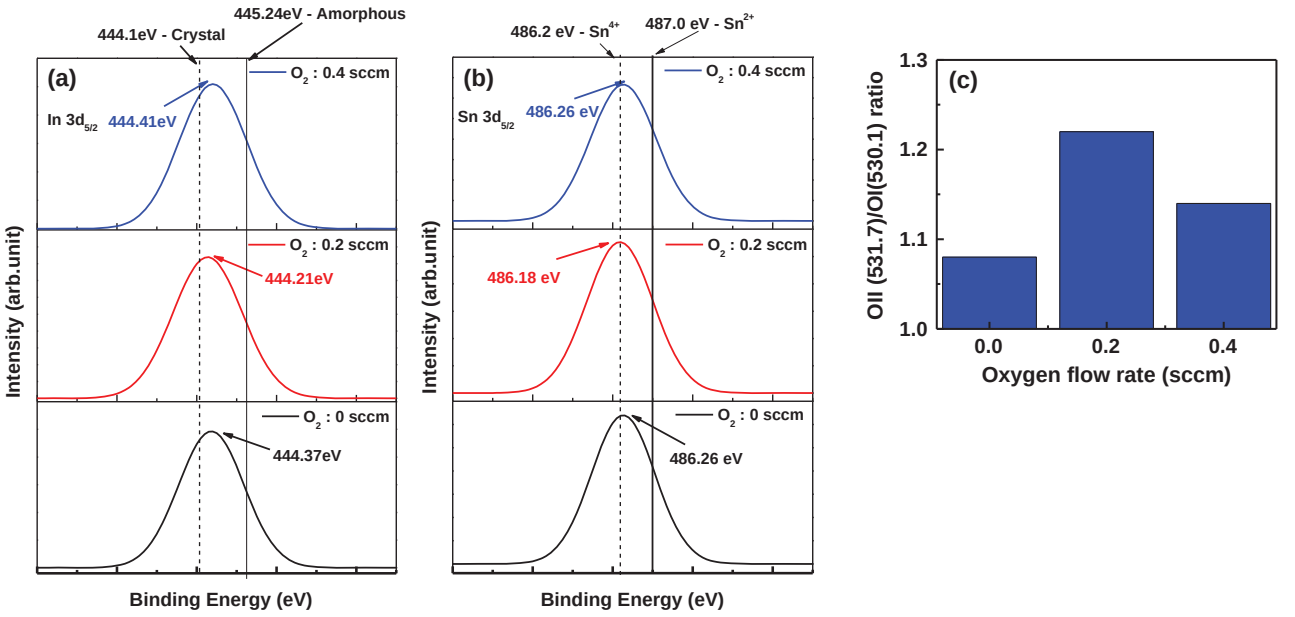

Fig. 4. The XPS spectra showing the variation of (a) In $3d_{5/2}$, (b) $Sn_{5/2}$, and (c) the ratio of O_{II}/O_I for different oxygen flow rates. The process conditions are the same as those in Figure 3.

the highest as 1.2 at the oxygen flow rate of 0.2 sccm indicating that the deposited film has higher concentration of oxygen vacancies than other conditions. In the ITO film, the oxygen vacancies are related to the electrical carriers, therefore, for the ITO film with the oxygen flow rate of 0.2 sccm, as shown in Figure 3(a), the high carrier concentration was obtained not only by the doping of Sn^{4+} but also by the high oxygen vacancy in the film.

For the optimized process condition of 0.2 sccm oxygen flow rate in Figure 4, the electrical properties of ultra-thin ITO film were measured for different thickness of ITO film from 10 to 50 nm in thickness and the results are shown in Figure 5(a) for resistivity and Figure 5(b) for other electrical properties such as resistivity, carrier concentration, and mobility. As shown in Figure 5(a), the sheet resistance was rapidly decreased from 1034 to 178 Ω/sq with increasing the thickness from 10 to 30 nm and the further increase of thickness to 50 nm decreased the resistivity slowly to 115 Ω/sq. The decrease of sheet resistance with increasing the ITO thickness is related to the increased ITO thickness but also can be related to the improved crystallinity of the ITO film with increasing the thickness. As shown in Figure 5(b), the increase of ITO film thickness also significantly decreased the resistivity from 1.24×10^{-3} to 5.2×10^{-4} Ω · cm with increasing the thickness from 10 to 30 nm and the further increase in thickness to 50 nm slowly decreased the resistivity. Therefore, it suggests that the crystallinity of the deposited ultra-thin ITO film was improved significantly up to 30 nm and the further increase of the ITO film thickness to 50 nm was less significantly improved the crystallinity.

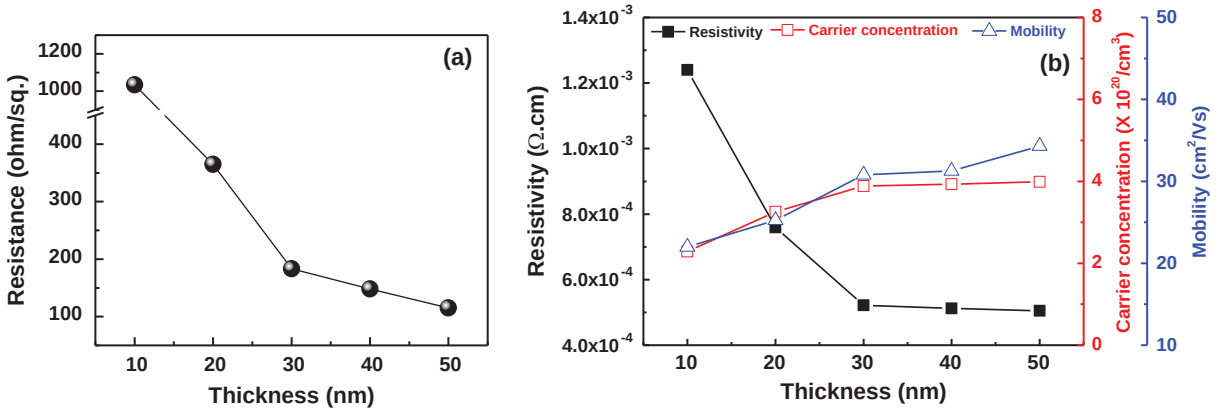

Fig. 5. (a) The sheet resistance and (b) other electrical properties (resistivity, carrier concentration, and mobility) of the ultra-thin ITO films as a function of thickness for 0.2 sccm of oxygen flow rate. The other conditions are the same as those in Figure 3.

The optical properties of the ultra-thin ITO films deposited on soda lime glass substrates with the different thicknesses in Figure 5 were observed and the results are shown in Figure 6(a). The inset figure shows the optical transmittances of ITO films averaged from 400 to 800 nm. The soda lime glass substrate itself showed the optical transmittance of ~90% for the visible wavelength range of 400~800 nm and the deposition of ITO films decreased the optical transmittance with the increase of ITO thickness. However, the optical transmittance of the ITO films deposited on the soda lime glass substrate with the thickness from 30 to 50 nm was in the range from 86 to 80% for the visible wavelengths, and which is suitable for optical device applications.[1,28] Figure 6(b) shows the variation of substrate temperature measured during the operation of L-3DMS using the condition in Figure 5 up to 1,200 seconds. As shown in Figure 6(b), the substrate temperature was increased with increasing deposition time due to no intentional temperature control and was almost saturated after ~300 seconds. For the deposition of 50 nm thick ITO film, it takes about 26 seconds for deposition, therefore, the substrate temperature was lower than 100 °C for the deposition thickness ≤50 nm.

Table I shows the performance overview of the ITO thin films deposited by various methods for the thickness of ≤200 nm.[30–33] As shown in Table I, most of the processing methods are involved with the substrate temperature higher than 100 °C. Among these, the atomic layer deposition[31] showed the lowest resistivity at the thickness of 40 nm, however, this method needs longer processing time due to the low deposition rate in addition to a high substrate temperature. Also, the ion beam sputtering[13] also exhibited a good conductivity by showing the resistivity as low as 3×10^{-4} Ω·cm even though the thickness was thick as 200 nm and the optical transmittance is a little low. Compared to these methods, the present work with L-3DMS

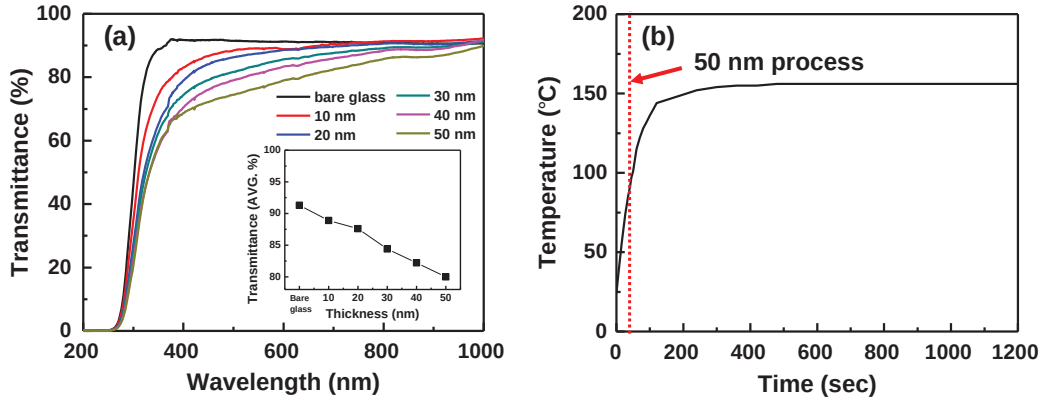

Fig. 6. (a) Variation of optical transmittance and average transmittance (400–800 nm, inset figure) of the ultra-thin ITO films for different thickness. (b) Substrate temperature measured during the operation of L-3DMS using the condition in Figure 5 up to 1,200 sec.

Table I. Comparison of thin (≤200 nm) ITO film performances deposited by various methods.

Deposition methods	Film thickness (nm)	Substrate (T_S) temperature (°C)	s = Sheet resistance (Ω/sq.) ρ = Film resistivity (Ωcm)	Mobility (cm^2/Vs)	Transmittance (%)	Remark
MS[29,30]	25–200[31]; 200[32]	T_s = 100–230 and T_a = 100[30]; T_S < 100[31]	$\rho = 2.5\times^4$; s = 30 – 85	30; –	75–92[30] 84–88[31]	Substrate heating and post annealing; Small area process; Thick thickness
Dual pulsed Magnetron source[32]	50	T_S > 120	$\rho = 9 \times 10^4$	13	85–88	High temperature process; Not good electrical property
Facing target Magnetron sputtering[34]	40	T_s = 300	ρ = 3–8 × 10^4	15–20	80–90	High temperature process
Atomic layer deposition (ALD)[31]	40	T_s = 150–275	$\rho = 2.0 \times 10^2$–5.3×10^5	0.5–13	80–90	Very low growth Rate; High temperature process
Ion beam sputtering (IBS)[13]	200	$T_s = 40 - 200$	$\rho = 1.5 - 3 \times 10^4$	20–25	75–85	Small area process; High temperature process
3DMS (Present work)	30–50	T_s < 100	$\rho = 5.4 \times 10^4$ $s = 170 \pm 20$	32–35	80–86	Option of larger area process that can be scaleable

showed relatively higher electrical/optical performances at the ultra-thin thickness (<50 nm) at the temperature lower than 100 °C compared to other methods, and which can be applicable to flexible substrates.

4. CONCLUSIONS

Highly conductive and highly optically transparent ultra-thin ITO thin films were deposited at the substrate temperature lower than 100 °C by using the L-3DMS which has a high plasma density and a low plasma potential due to highly confined magnetic fields in the plasma source. Due to the plasma density higher than 4×10^{11} cm^{-3} and the plasma potential lower than 7 V, a highly crystalline ITO films with high oxygen vacancies could be deposited for the ultra-thin ITO film thickness (≤50 nm) by controlling the oxygen flow rate to Ar, and which resulted in a high carrier concentration in the film. By optimizing the oxygen flow rate, a highly transparent (86% in the visible wavelengths including~90% optical transmittance of soda lime glass substrate) and highly conductive (resistivity: $\sim 5 \times 10^{-4}$ $\Omega \cdot cm$, carrier concentration: 3.8×10^{20} cm^3, and mobility: 31 cm^2/Vs) ultra-thin (30 nm) ITO film could be deposited by the L-3DMS for the oxygen flow rate of 0.2 sccm to 4 mTorr Ar at the temperature lower than 100 °C. It is believed that the ultra-thin ITO film deposited by the L-3DMS can be applicable to various flexible optical devices as a transparent conductive film.

Conflicts of Interests

The authors declare no conflict of interests.

Acknowledgments: This work was supported by the Korea Institute of Energy Technology Evaluation and Planning (KETEP) and the Ministry of Trade, Industry & Energy (MOTIE) of the Republic of Korea (20202010100020).

References and Notes

1. H. Kim, A. Piqué, S.J. Horwitz, H. Mattoussi, Z. Murata, H. H. Kafafi, and D. B. Chrisey, Indium tin oxide thin films for organic lightemitting devices. *Appl. Phys. Lett.* 74, 3444 **(1999)**.
2. R. G. Gordon, Criteria for choosing transparent conductors. *MRS Bull.* 25, 52 **(2000)**.
3. K. H. Choi, J. Kim, Y. J. Noh, S. I. Na, and H. K. Kim, Ag nanowire-embedded ITO films as a near-infrared transparent and flexible anode for flexible organic solar cells. *Solar Energy Matererials and Solar Cells* 110, 147 **(2013)**.
4. K. S. Tseng and Y. L. Lo, Effect of sputtering parameters on optical and electrical properties of ITO films on PET substrates. *Appl. Surf. Sci.* 285, 157 **(2013)**.
5. L. álvarez-Fraga, F. Jiménez-Villacorta, J. Sánchez-Marcos, A. De Andrés, and C. Prieto, Indium-tin oxide thin films deposited at room temperature on glass and PET substrates: Optical and electrical properties varition with the H_2-ar sputtering gas mixture. *Appl. Surf. Sci.* 344, 217 **(2015)**.
6. S. H. Park, S. J. Lee, J. H. Lee, J. Kal, J. Hahn, and H. K. Kim, Large-area roll-to-roll sputtering of transparent ITO/Ag/ITO cathodes for flexible inverted organic solar cell modules. *Org. Electron.* 30, 112 **(2016)**.
7. C. Guillén and J. Herrero, Sturcture, optical, and electrical properties of indium tin oxide thin films prepared by sputtering at room temperature and annealed in air or nitrogen. *Journal of Applied Physsics* 101, 073514 **(2007)**.
8. C. Liu, T. Matsutani, T. Asanuma, K. Murai, M. Kiuchi, E. Alves, and M. Reis, Room-temperature growth of crystalline indium tin oxide films on glass using low-energy oxygen-ion-beam assisted deposition. *J. Appl. Phys.* 93, 2262 **(2003)**.
9. H. C. Lee and O. O. Park, Electron scattering mechanisms in indium-tin-oxide thin films: Grain boundary and ionized imprity scattering. *Vacuum* 75, 275 **(2004)**.
10. H. Omoto, A. Takamatsu, and T. Kobayashi, Effect of substrate temperature on tin-doped indium oxide films deposited by dc arc discharge ion plating. *Vacuum* 80, 783 **(2006)**.
11. A. S. A. C. Diniz and C. J. Kiely, Crystallisation of indium-tin-oxide (ITO) thin films. *Renewable Energy* 29, 2037 **(2004)**.
12. J. H. Kim, K. A. Jeon, G. H. Kim, and S. Y. Lee, Electrical, structural, and optical properties of ITO thin films prepared at room temperature by pulsed laser deposition. *Appl. Surf. Sci.* 252, 4834 **(2006)**.
13. D. Kim, Y. Han, J. S. Cho, and S. K. Koh, Low temperature deposition of ITO thin films by ion beam sputtering. *Thin Solid Films* 377–378, 81 **(2000)**.
14. H. El Rhaleb, E. Benamar, M. Rami, J. P. Roger, A. Hakam, and A. Ennaoui, *Appled Surface Science* 201, 138 **(2002)**.
15. H. R. Fallah, M. Ghasemi, A. Hassanzadeh, and H. Steki, The effect of annealing on structural, electrical and optical properties of nanostructured ITO films propared by e-beam evaporation. *Mater. Res. Bull.* 42, 487 **(2007)**.
16. S. S. Kim, S. Y. Choi, C. G. Park, and H. W. Jin, Transparent conductive ITO thin films through the sol-gel process using metal salts. *Thin Solid Films* 347, 155 **(1999)**.
17. Y. C. Park, Y. S. Kim, H. K. Seo, S. G. Ansari, and H. S. Shin, ITO thin films deposited at different oxygen flow rates on Si(100) using the PEMOCVD method. *Surf. Coat. Technol.* 161, 62 **(2002)**.
18. W. Deng, T. Ohgi, H. Nejo, and D. Fujita, Development of conductive transparent indium tin oxide (ITO) thin films deposited by direct current (DC) magnetron sputtering for photon-STM applications. *Applied Physics a Materials Science and Processing* 72, 595 **(2001)**.
19. Y. Hu, X. Diao, C. Wang, W. Hao, and T. Wang, Effects of heat treatment on properties of ITO films prepared by rf magnetron sputtering. *Vacuum* 75, 183 **(2004)**.
20. L. Wen, B. B. Sahu, and J. G. Han, Development and utility of a new 3-D magnetron source for high rate deposition of highly conductive ITO thin films near room temperature. *PCCP* 20, 4818 **(2018)**.
21. B. B. Sahu, L. Wen, and J. G. Han, Highly conductive flexible ultra thin ITO nanoclusters prepared by 3-D confined magnetron sputtering at a low temperature. *Scripta Mater.* 149, 98 **(2018)**.
22. B. B. Sahu, L. Wen, J. H. Kwon, and J. G. Han, Factors affecting the properties of highly conductive flexible ultrathin ITO films in confined large area magnetron sputtering in three dimensions. *AIP Advances* 8, 105112 **(2018)**.
23. B. B. Sahu, J. G. Han, H. R. Kim, K. Ishikawa, and M. Hori, Experimental evidence of warm electron populations in magnetron sputtering plasma. *J. Appl. Phys.* 117, 033301 **(2015)**.
24. O. Baranov, M. Romanov, M. Wolter, S. Kumar, X. Zhong, and K. Ostrikov, Low-pressure planar magnetron discharge for surface deposition and nanofabrication. *Physics of Plasmas* 17, 053509 **(2010)**.
25. M. Marikkannan, M. Subramanian, J. Mayandi, M. Tanemura, V. Vishnukanthan, and J. M. Pearce, Effect of ambient combinations

of argon, oxygen, and hydrogen on the properties of DC magnetron sputtered indium tin oxide films. *AIP Advances* 5, 017128 **(2015)**.

26. Y. S. Kim, Y. C. Park, S. G. Ansari, B. S. Lee, and H. S. Shin, Effect of substrate temperature on the bonded states of indium tin oxide thin films deposited by plasma enhanced chemical vapor deposition. *Thin Solid Films* 426, 124 **(2003)**.

27. W. F. Wu and B. S. Chiou, Effect of oxygen concentration in the sputtering ambient on the microstructure, electrical and optical properties of radio-frequency magnetron-sputtered indium tin oxide films. *Semicond. Sci. Technol.* 11, 196 **(1996)**.

28. J. S. Kim, P. K. H. Ho, D. S. Thomas, R. H. Friend, F. Cacialli, G. W. Bao, and S. F. Y. Li, X-ray photoelectron spectroscopy of surface-treated induium-tin oxide thin films. *Chem. Phys. Lett.* 315, 307 **(1999)**.

29. K. Ellmer, Past achievements and future challenges in the development of optically transparent electrodes. *Nat. Photonics* 6, 809 **(2012)**.

30. C. David, B. P. Tinkham, P. Prunici, and A. Panckow, Highly conductive and transparent ITO films deposited at low temperatures by pulsed DC magnetron sputtering from ceramic and metallic rotary targets. *Surf. Coat. Technol.* 314, 113 **(2017)**.

31. M. Laurenti, S. Bianco, M. Castellino, N. Garino, A. Virga, C. F. Pirri, and P. Mandracci, Toward plastic smart windows: Optimiztion of indium tin oxide electrodes for the synthesis of electrochromic devices on polycarbonate substrates. *ACS Applied Materials and Interfaces* 8, 8032 **(2016)**.

32. W. J. Maeng, D. W. Choi, K. B. Chung, W. Koh, G. Y. Kim, S. Y. Choi, and J. S. Park, Highly conducting, transparent, and flexible indium oxide thin film prepared by atomic layer deposition using a new liquid precursor $Et_2InN(SiMe_3)_2$. *ACS Applied Materials and Interfaces* 6, 17481 **(2014)**.

33. S. Il Kim, K. W. Lee, B. B. Sahu, and J. G. Han, Flexible OLED fabrication with ITO thin film on polymer substrate. *Japanes Journal of Applied Physics* 54, 09030 **(2015)**.

34. J. Gwamuri, A. Vora, J. Mayandi, D. Güney, P. L. Bergstrom, and J. M. Pearce, A new method of proparing highly conductive ultra-thin indium tin oxide for plasmonic-enhances thin film solar photovoltaic devices. *Sol. Energy Mater. Sol. Cells* 149, 250 **(2016)**.

ARTICLE